

11-2-2015

Determination of the Gelation Mechanism of Freeze–Thawed Hen Egg Yolk

Carmen Au

Iowa State University

Nuria C. Acevedo

Iowa State University, nacevedo@iastate.edu

Harry T. Horner

Iowa State University, hth@iastate.edu

Tong Wang

Iowa State University, tongwang@iastate.edu

Follow this and additional works at: http://lib.dr.iastate.edu/fshn_hs_pubs

 Part of the [Food Chemistry Commons](#), [Food Microbiology Commons](#), [Genetics Commons](#), and the [Human and Clinical Nutrition Commons](#)

The complete bibliographic information for this item can be found at http://lib.dr.iastate.edu/fshn_hs_pubs/13. For information on how to cite this item, please visit <http://lib.dr.iastate.edu/howtocite.html>.

This Article is brought to you for free and open access by the Food Science and Human Nutrition at Iowa State University Digital Repository. It has been accepted for inclusion in Food Science and Human Nutrition Publications by an authorized administrator of Iowa State University Digital Repository. For more information, please contact digirep@iastate.edu.

Determination of the Gelation Mechanism of Freeze–Thawed Hen Egg Yolk

Abstract

A study of yolks stored up to 168 d at $-20\text{ }^{\circ}\text{C}$ was conducted to determine the gelation behavior and mechanism of freeze–thawed yolk. Methods used were rheology, native and sodium dodecyl sulfate polyacrylamide gel electrophoresis (native- and SDS-PAGE), differential scanning calorimetry (DSC), transmission electron microscopy (TEM), particle size analysis, and proton nuclear magnetic resonance (^1H NMR) spectroscopy for matrix mobility. Results indicate that both constituents of plasma and granules contributed to gelation of yolk under freezing. PAGE analyses suggest that granular proteins participated in aggregation during freeze–thaw. Increasing gel strength and particle size and decreasing water and lipid–water mobility indicate that lipoproteins or apolipoproteins aggregated. At storage times ≥ 84 d, increased protein and lipid mobility, the detection of smaller particles, and secondarily increased gel strength suggest the liberation of protein or lipoprotein components from previously formed aggregates and further aggregation of these constituents. Disruption of the gelled yolk matrix observed with TEM supported that ice crystal formation was required for gelation to occur. A two-stage dynamic gelation model is thus proposed.

Keywords

egg yolk, frozen storage, gelation, lipoproteins

Disciplines

Food Chemistry | Food Microbiology | Food Science | Genetics | Human and Clinical Nutrition

Comments

Reprinted (adapted) with permission from *Journal of Agricultural and Food Chemistry*, 63(46); 10170-10180. Doi: [10.1021/acs.jafc.5b04109](https://doi.org/10.1021/acs.jafc.5b04109). Copyright 2015 American Chemical Society.

Determination of the Gelation Mechanism of Freeze–Thawed Hen Egg Yolk

Carmen Au,[†] Nuria C. Acevedo,^{*,†} Harry T. Horner,[‡] and Tong Wang^{*,†}

[†]Department of Food Science and Human Nutrition, Iowa State University, Ames, Iowa 50011, United States

[‡]Department of Genetics, Development and Cell Biology & Microscopy and NanoImaging Facility, Iowa State University, Ames, Iowa 50011, United States

S Supporting Information

ABSTRACT: A study of yolks stored up to 168 d at $-20\text{ }^{\circ}\text{C}$ was conducted to determine the gelation behavior and mechanism of freeze–thawed yolk. Methods used were rheology, native and sodium dodecyl sulfate polyacrylamide gel electrophoresis (native- and SDS-PAGE), differential scanning calorimetry (DSC), transmission electron microscopy (TEM), particle size analysis, and proton nuclear magnetic resonance (^1H NMR) spectroscopy for matrix mobility. Results indicate that both constituents of plasma and granules contributed to gelation of yolk under freezing. PAGE analyses suggest that granular proteins participated in aggregation during freeze–thaw. Increasing gel strength and particle size and decreasing water and lipid–water mobility indicate that lipoproteins or apolipoproteins aggregated. At storage times ≥ 84 d, increased protein and lipid mobility, the detection of smaller particles, and secondarily increased gel strength suggest the liberation of protein or lipoprotein components from previously formed aggregates and further aggregation of these constituents. Disruption of the gelled yolk matrix observed with TEM supported that ice crystal formation was required for gelation to occur. A two-stage dynamic gelation model is thus proposed.

KEYWORDS: egg yolk, frozen storage, gelation, lipoproteins

INTRODUCTION

Food processors use hen egg yolk as a highly nutritional and functional ingredient in a variety of products, such as mayonnaise, salad dressings, cakes, and custards.¹ Yolks are frozen for increased shelf life (up to 1 yr) and for ease of transport and storage.² However, after freezing (at $\leq -6\text{ }^{\circ}\text{C}$) and thawing of yolk, an undesirable phenomenon termed gelation occurs.³ Gelation is an irreversible loss of fluidity which results in reduced yolk functionality and dispersibility.⁴ The food industry practices the addition of 2–10% salt, sugar, or corn syrup to yolk (as a cryoprotectant) to minimize gelation.⁵ Yolk gelation has been studied extensively, as reported mostly 20–30 year ago; however, none of the previous studies systematically reports and relates all changes that occur during such gelation. Thus, the mechanism proposed may be partial. Methods based on newer technology and relating multiple analyses and observations may add new knowledge of the mechanism of yolk gelation.

Despite extensive research on freeze–thaw gelation of yolk, its mechanism has not been fully elucidated. This is largely due to the conflicting results reported by many groups of researchers. The most popular explanation of the yolk gelation mechanism is the aggregation of low-density lipoproteins (LDL) of yolk plasma.^{6–10} However, there is a disagreement on the mechanism of LDL aggregation. Telis and Kieckbusch⁶ proposed that the breaking of LDL micelles is the first step of gelation, and as freezing progresses, dehydration of apolipoproteins leads to LDL aggregation. Kurisaki et al.⁷ suggested that, during freeze–thaw, surface components of LDL are liberated and the newly exposed sites participate in aggregation. Wakamatu et al.⁸ disagreed, attributing LDL aggregation to

conformational changes of LDL, not liberation of LDL components. Kumar and Mahadevan⁹ and Mahadevan et al.¹⁰ suggested that LDL aggregation is a result of the interaction of protein molecules after disruption of lecithin–protein interactions.

The majority of studies emphasized the role of plasma LDL and/or only studied plasma LDL to determine the mechanism of yolk gelation.^{6,7,9–12} A few studies considered the role of granules in the gelation mechanism. Wakamatu et al.⁸ indicated that they could not exclude granular LDL (LDLg) in the participation of LDL aggregation because the lipid compositions of plasma and granules LDL were very similar. Chang et al.¹³ proposed that liberated LDLg contributed to yolk gelation. Powrie et al.⁴ also suggested that an interaction between granules and plasma LDL led to gelation. To summarize these previous studies, many different proposed mechanisms of yolk gelation exist, yet most researchers agreed that removal of water via ice crystal formation is necessary for gelation to occur.

The objective of this research was to determine more precisely the gelation behavior and gelation mechanism of freeze–thawed hen egg yolk with all available traditional and newer techniques and, more importantly, the kinetics of these changes. The gained knowledge can be used to develop techniques to reduce or prevent gelation without the use of salt or sugar for the production of low-sodium, low-sugar, or sugar-free foods containing freeze–thawed yolk. We hypothesized

Received: August 21, 2015

Revised: October 28, 2015

Accepted: November 2, 2015

Published: November 2, 2015

that gelation occurs via aggregation of all yolk components. Aggregation is a result of two factors: disruption of lipoprotein particle surfaces and concentration of yolk components due to formation of large ice crystals during freezing. The formation of large ice crystals via slow cooling is required, as it has been proven that gelation does not occur with supercooling of yolk in liquid nitrogen or oxygen.^{10,14} Large ice crystal formation removes water that is necessary for the structural integrity of the LDL phospholipid monolayer.¹⁵ Hydrophobic regions which were previously inaccessible can become available to participate in protein–protein interactions after dehydration. It was also hypothesized that granules or components of granules participate in gelation by providing additional stabilizing force in the gel network. Thus, it is important to study the whole yolk, not just the plasma fraction, to determine the gelation behavior and mechanism.

Past research showed that the properties of yolk-containing products were affected by the use of yolks frozen for varying lengths of time up to 120 d.¹⁶ In this study, fresh and gelled yolk (stored at $-20\text{ }^{\circ}\text{C}$ for 0, 1, 3, 7, 14, 28, 84, and 168 d and thawed) were examined to determine the effect of varying frozen storage times on yolk gelation. Preliminary results indicated that frozen storage time had an effect on gelation. This research focused on physical and chemical analyses of fresh and gelled yolk, and these methods included the study of gel mechanical properties with small deformation rheology, particle size distribution by particle size analysis, matrix mobility via proton nuclear magnetic resonance (^1H NMR) spectroscopy, protein changes by native and sodium dodecyl sulfate polyacrylamide gel electrophoresis (Native- and SDS-PAGE), water changes by differential scanning calorimetry (DSC), and microstructural rearrangement with transmission electron microscopy (TEM). Several of the aforementioned methods have not previously been used to study yolk freeze–thaw gelation.

MATERIALS AND METHODS

Materials. Grade A large white shell eggs were purchased from retailers in Ames, IA at least 14 d before the sell-by date, i.e., 30 d after the packing date. Eggs were held for no more than 16 d in refrigeration temperature ($4\text{ }^{\circ}\text{C}$) during transportation as well as storage at the retailer and at the research laboratory.

Egg yolk separation. Yolks were separated using a modified version of the method by Powrie et al.⁴ Yolks were separated from the albumen, and the chalazae were carefully removed from yolk. The yolk with intact vitelline membrane was washed carefully and each yolk was rolled on a sheet of paper towel to remove remaining water and albumen. The vitelline membrane was pierced and yolk was drained into beaker. After completing the yolk harvest from at least six eggs, the yolks in the beaker were stirred slowly for 1 min to ensure sample homogeneity. Yolks were frozen immediately or stored in a $4\text{ }^{\circ}\text{C}$ refrigerator for no more than 24 h before freezing.

Yolk freezing and thawing. For all analyses excluding rheological tests, 100 mL of yolk was poured in 10 mL portions into ten 25 mL polystyrene vials with snap-on lids. Up to five vials were vacuum sealed in a vacuum bag with a FoodSaver V222 vacuum sealing system (SunBeam Products, Inc., Jarden Consumer Solutions, Boca Raton, FL) to reduce freezer dehydration or burn. The vacuum-sealed bags of yolk vials were submerged in the reservoir of a Haake SC 100 refrigerated/heated bath circulator (Thermo Fisher Scientific, Waltham, MA) filled with 1:1 ethylene glycol:Milli-Q water at $0\text{ }^{\circ}\text{C}$. The bath was then set to $-20\text{ }^{\circ}\text{C}$. After the samples reached $-20\text{ }^{\circ}\text{C}$ at a cooling rate of $0.3\text{--}0.5\text{ }^{\circ}\text{C}/\text{min}$, the yolks were held in the $-20\text{ }^{\circ}\text{C}$ bath for 3 h. The frozen yolks were stored in a $-20 \pm 2\text{ }^{\circ}\text{C}$ freezer for the designated amount of time (1, 3, 7, 14, 28, 84, and 168 d). Yolks were transferred from the freezer to thaw for 1 h in a $25\text{ }^{\circ}\text{C}$ Neslab

GP-300 water bath (Neslab Instruments, Inc., Portsmouth, NH). Gelled yolks were analyzed immediately after thawing. Fresh yolks were analyzed no later than 6 h after separation, and if storage was required the yolks were kept at $4\text{ }^{\circ}\text{C}$ until analysis.

Gelled yolk samples for rheological tests were prepared differently. Yolk disks (35 mm diameter, 3 mm thickness) were prepared in an aluminum mold plate (23.2 cm length, 7.2 cm width, 3 mm height) with five circles of 35 mm-diameter cutouts. A custom aluminum apparatus composed of two heat transfer blocks (23.2 cm length, 7.2 cm width, 2.5 cm height), as shown in Figure 1, was connected with

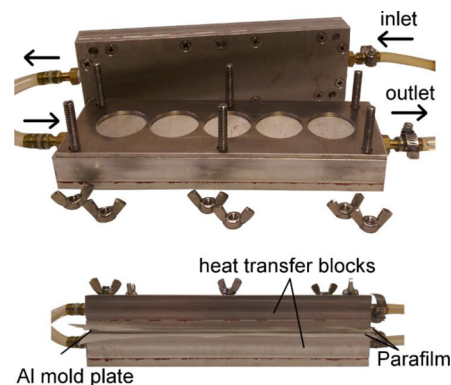


Figure 1. Heat transfer apparatus used to prepare frozen yolk disks.

plastic tubing to the inlet and outlet ports of the Haake SC 100 refrigerated/heated bath circulator. A 1:1 ethylene glycol:Milli-Q water mixture was circulated through the blocks using the Haake SC 100 bath. When the refrigerated bath reached $0\text{ }^{\circ}\text{C}$, a sheet of Parafilm (Beemis Company, Inc., Oshkosh, WI) was placed over the bottom block. The five cutouts were filled with raw egg yolk, and another sheet of Parafilm was used to cover the mold plate. The top heat transfer block was quickly fitted over the filled mold plate. The cooling bath was set to $-20\text{ }^{\circ}\text{C}$ immediately after depositing the yolk and assembling the apparatus. After reaching $-20\text{ }^{\circ}\text{C}$ at a cooling rate of $0.3\text{--}0.5\text{ }^{\circ}\text{C}/\text{min}$, the yolks were held in the apparatus for 3 h. The mold plate and two Parafilm sheets were then removed from the blocks and vacuum sealed in a vacuum bag to reduce freezer burn. The samples were stored in a $-20 \pm 2\text{ }^{\circ}\text{C}$ freezer for the designated amount of time (1, 3, 7, 14, 28, 84, and 168 d).

On the day of analysis, control samples were prepared. Raw yolk cannot be used for the type of rheological test used in this study due to its high fluidity. A 0 d gelled yolk was used as the control. This control was prepared as above, but rheological measurements were made immediately after the $-20\text{ }^{\circ}\text{C}$ 3 h holding period. The 0 d gelled yolk control was included in tests utilizing instruments with high sensitivity to the changes: particle size analysis, matrix mobility measurements, and free water experiments.

Egg yolk fractionation. Whole fresh yolk and gelled yolk (7d frozen) samples were fractionated into plasma and granules with a method modified from McBee and Cotterill¹⁷ and Anton.¹⁸ Mixtures of 1:1.5 (v/v) yolk:Milli-Q water were prepared in beakers and stirred on a stir plate for 1.5 h. Then, 35 mL of the yolk:water mixture was aliquoted to 50 mL conical polypropylene centrifuge tubes. The tubes were transferred to a FIBERLite F15–8x-50cy fixed angle rotor in a Sorvall Legend XT centrifuge (Thermo Fisher Scientific, Osterode, Germany) and centrifuged at $10,000g$ for 45 min at $4\text{ }^{\circ}\text{C}$. The plasma, or supernatant, was collected and centrifuged again with the same parameters. The plasma was collected for analysis after the second centrifugation. Only the granules, or pellet, from the first centrifugation was used for analysis. Both fractions were stored in capped tubes at $4\text{ }^{\circ}\text{C}$ for no more than 12 h before PAGE sample preparation and analysis.

Whole yolk and yolk plasma delipidation. Lipids which may interfere with protein separation by PAGE were removed from whole yolk and yolk plasma using the method of Cham and Knowles.¹⁹

Aliquots of yolk or plasma of 5 mL were placed in 50 mL conical polypropylene centrifuge tubes, and 10 mL of 1:1.5 (v/v) analytical grade 1-butanol:di-isopropyl ether (B-DIPE) (Fisher Scientific, Pittsburgh, PA) was added. The tubes were mixed for 30 min on a Thermolyne Roto Mix Type 50800 Shaker (Barnstead International, Dubuque, IA), then centrifuged using an Eppendorf A-4-62 rotor in an Eppendorf 5810-R centrifuge (Eppendorf AG, Hamburg, Germany) at 500g for 5 min at 25 °C. The top organic layer with dissolved lipids was removed with a glass Pasteur pipet and discarded. The bottom aqueous layer was centrifuged again with the same conditions, and the remaining organic layer was discarded. The delipidated samples were capped and stored at 4 °C no more than 12 h before PAGE sample preparation and analysis.

Rheological analysis. After frozen storage, the yolk samples were prepared for rheological analysis using a Haake RS 150 rheometer (Gebrüder HAAKE, Karlsruhe, Germany). The sample disk was removed from the aluminum mold plate one at a time. Only after thawing and completion of the test was another disk removed from the plate for testing. A polyvinyl chloride (PVC) cylindrical plunger (35 mm diameter, 62 mm height) was used to push the disk out of the mold and onto square of type 60 coarse sandpaper (3M, St. Paul, MN) to thaw on a benchtop at room temperature for 15 min. In preliminary tests, a noticeable film formed across the disk surface after 17 min due to drying. After the 15 min thaw, the disk and sandpaper were transferred and the sandpaper was fixed to the rheometer platform with packing tape. The use of sandpaper and the serrated plate ensured accurate measurement of the samples since slipping of the sample on either side of the disk was prevented.

One control (C_{0d}) and seven treatments (1, 3, 7, 14, 28, 84, 168 d) were measured using the rheometer. Eight disks (replicates) per sample were subjected to an oscillatory stress sweep to test yolk properties. The serrated parallel plate descended to a gap of 3.05 mm, the distance from the sandpaper to the plate, at which the plate just touches the surface of the disk. The disk must not be deformed at this point, since material pushed out from under the plate distorts readings. A 10–300 Pa stress sweep was performed with a 35 mm-diameter serrated titanium parallel plate (Gebrüder HAAKE, Karlsruhe, Germany) at a frequency of 1 Hz with 40 steps (data points). The platform temperature was regulated at a constant 20 °C by a Thermo Haake F6–C25 refrigerated circulator bath and TC-81 Peltier temperature system (Gebrüder HAAKE, Karlsruhe, Germany) connected to the rheometer. The average elastic modulus, G' , within the linear viscoelastic range (LVR) was reported as it correlates with gel hardness. The LVR is the period in which G' is constant and the material acts as a solid. The point at which the material deforms is the yield stress, σ^* , another measurement of gel strength. Yield stress is the amount of stress required to induce flow and was calculated as the stress at which a 10% reduction in the average G' of LVR was achieved.

Particle size analysis. Particle size distributions of fresh and gelled yolk were measured using an angular light scattering, or laser diffraction (LD) method. Two controls, fresh yolk and 0 d gelled yolk (C_F , C_{0d}), and seven treatments (1, 3, 7, 14, 28, 84, 168 d) were measured in triplicate using a Malvern Mastersizer 2000 particle size analyzer with Hydro 2000 MU large volume wet sample dispersion unit (Malvern Instruments, Inc., Worcestershore, UK). Plasma and granule fractions of the fresh yolk control were also measured to identify the populations detected in the particle size distribution of whole fresh yolk. All samples were diluted 1:1.5 (v/v) sample:Milli-Q water and mixed for 1.5 h on a stir plate until homogeneous. Diluted samples were added dropwise to a 2 L-beaker of deionized water used with the wet sample dispersion unit. Measurements were made when obscurations of 10–15% were reached. Obscuration is the fractional loss of light intensity when compared with the intensity taken during a background measurement.²⁰ Two refractive indices (RI) were used in the measurements: the RI of the water/background, 1.00, and the RI of the yolk/sample, 1.42.²¹ Percentile diameters $d(0.1)$, $d(0.5)$, and $d(0.9)$ were reported and indicate that 10, 50, and 90%, respectively, of the volume distribution was below that diameter. The surface area moment mean or De Brouckere Mean Diameter, $D[3, 2]$, and the volume

moment mean or De Brouckere Mean Diameter, $D[4, 3]$, were also reported.

Matrix mobility determination. Two controls, fresh yolk and 0 d gelled yolk (C_F , C_{0d}), and seven treatments (1, 3, 7, 14, 28, 84, 168 d) were measured for their matrix mobility using a Bruker Minispec mq-20 ^1H NMR spectrometer (Bruker BioSpin Corporation, Billerica, MA). Flat-bottom glass NMR tubes (10 mm diameter, 180 mm length) were prepared in triplicate for each sample. Six runs were completed for each tube for a total of 18 measurements per sample. Tubes were filled with yolk samples to a height of 4 cm and capped. Immediately before measurement, capped samples were held at 20 °C in a Duratech TCON 2000 high precision dry bath system (Duratech, Carmel, IN) for 60–70 min. The probe head was regulated at a constant temperature of 20 °C by a Julabo F25-ED refrigerated/heated circulator (Julabo GmbH, Seelbach, Germany) connected to the minispec.

The Carr–Purcell–Meiboom–Gill (CPMG) pulse sequence was used to measure T_2 between 0.2 and 1000 millisecond (ms). The separation between the 90° and 180° pulse was 2.28 microsecond (μs) and 4.98 μs , respectively, and 600 data points were collected. For CPMG measurements, 8 scans were made with a 15.0 s recycle delay. Relaxation curves were fitted to a continuous distribution of exponentials using the Inverse Laplace Transformation (ILT) algorithm (Bruker software, Bruker BioSpin Corporation, Billerica, MA), also referred to as the CONTIN algorithm of Provencher.²² T_2 is reported for each peak in ms. Proton populations (PP), or areas of the peaks, are proportional to the relative quantities of yolk component and are expressed in percentage (%) normalized for each sample. Proton populations were normalized by transforming the peak areas into percentages where the sum of all peaks was 100%.

Free water measurement. Differential scanning calorimetry (DSC) was performed on two controls, fresh yolk and 0 d gelled yolk (C_F , C_{0d}), and seven treatments (1, 3, 7, 14, 28, 84, 168 d) with a PerkinElmer PYRIS Diamond differential scanning calorimeter with HyperDSC (PerkinElmer Inc., Waltham, MA). Exothermic and endothermic transition heats of 2–5 mg of sample in standard aluminum hermetic pans with sealed lids were measured in triplicate. Scanning conditions were modified from Kamat et al.²³ and Wakamatu et al.²⁴ Each sample was held for 1 min at 25 °C, cooled to –30 °C at 10 °C/min rate and held at that temperature for 1 min, then heated from –30 to 25 °C at 10 °C/min rate.

Peak temperature and the heat of fusion, or change in enthalpy (ΔH), of exothermic and endothermic peaks were obtained. The amount of freezable or free water in yolk (g/g solid) was calculated as described by Wakamatu et al.²⁴ where the exothermic or endothermic heat was divided by the corresponding heat of fusion of pure water. Freezable water content is reported as the average of the exothermic and endothermic ΔH values. The heat of fusion of Milli-Q water used in freezable water calculations was measured using the aforementioned scanning parameters and was determined to be 215.09 ± 32.75 J/g for cooling and 253.69 ± 40.54 J/g for heating.

Protein characterization by gel electrophoresis. Proteins of one control, fresh yolk (C_F), and one treatment (7 d) were studied with Native and sodium dodecyl sulfate polyacrylamide gel electrophoresis (Native- and SDS-PAGE), which was performed according to Bio-Rad Laboratories (Hercules, CA) instructions and a method modified from Laca et al.²⁵ Only 7 d freeze–thawed yolk was analyzed with PAGE because in preliminary tests, no differences between 1, 3, 7, and 28 d treatments were observed. B-DIPE-delipidated whole yolk and yolk plasma were also studied, as preliminary results showed less protein band distortion in defatted yolk and plasma. Samples were diluted so that each gel lane held about 30 μg protein in 20 μL solution for Native-PAGE and 20 μg protein in 20 μL solution for SDS-PAGE. Protein concentration in egg yolk was determined using Bicinchoninic Acid (BCA) Protein Assay Kit according to the instruction of Pierce Biotechnology and Thermo Scientific instructions (Rockford, IL). Native-PAGE samples were diluted 1:2 (v/v) in Bio-Rad native sample buffer (glycerol, Tris, water), and SDS-PAGE samples were diluted 1:1 (v/v) in a mixture of 95% Bio-Rad Laemmli buffer (Tris-HCl, glycerol/bromophenol blue) and 5% β -mercaptoe-

thanol by volume. SDS-PAGE samples were heated in boiling water for 6 min. Electrophoresis of all samples was run on Bio-Rad Mini-PROTEAN TGX precast polyacrylamide gels (4–20% gel, 10-well comb, 30 μ L loading well) with the Mini-PROTEAN cell in an ice water bath. Bio-Rad Native running buffer (Tris/glycine/methanol/water) and SDS running buffer (Tris/glycine/SDS/water) were used.

The proteins were stained for 15 min with a solution consisting of 0.1% (w/v) Coomassie Brilliant Blue G-250 (Sigma-Aldrich Co, Kansas City, MO), 50% methanol, 10% acetic acid, and 40% Milli-Q water. The gels were destained overnight with multiple washes with a solution containing 10% acetic acid, 15% methanol, and 75% water. Precision Plus Protein Dual Color Standards (BioRad Laboratories, Inc., Hercules, CA) were used as protein standards. Three replicates of each gel were made, and the gels were scanned with an ImageScanner flatbed scanner (Amersham Pharmacia Biotech Inc., Piscataway, NJ). Gels with representative protein separation of each sample were processed with Image Processing and Analysis in Java software, ImageJ (National Institutes of Health, Bethesda, MD), for densitometric analysis. To allow comparison of proteins in different gels, scanned gel images were calibrated with an external standard following the NIH optical density calibration procedure.²⁶ Each lane was plotted as a density spectrum where each peak represented a protein band. The number of protein bands and the optical density, or peak area, of each band was determined. Density is reported in optical density units (OD).

Microstructure imaging by transmission electron microscopy (TEM). Fresh and gelled yolk samples were prepared TEM by encapsulating the yolk in 2% agar. One control, fresh yolk (C_F), and six treatments (1, 3, 7, 28, 84, 168 d) were studied with and without osmium tetroxide fixation. A total of 14 samples were prepared for imaging. Ten rectangular plugs (3 mm width, 4 mm length) were formed for each sample by placing small portions of yolk in cylindrical holes (2 mm diameter, 3 mm length) of a 2% agar Petri plate. The top of the filled holes were sealed with a thin layer of warm agar which was left to cool at room temperature. The agar was removed and plugs were cut to size with a razor blade. Further preparation of samples (e.g., fixation, staining, dehydration) were completed with a modified method of Mineki and Kobayashi.²⁷ After preparation, sections 60–90 nm thick were cut with a Leica UC6 ultramicrotome (Leeds Precision Instruments, Minneapolis, MN, USA) and placed on carbon film copper grids. The samples were imaged with a JEOL JEM-2100 200 kV scanning and transmission electron microscope (JEOL USA, Inc., Peabody, MA) using a Gatan ultrascan 1000 digital camera (Gatan, Inc., Pleasanton, CA) at Iowa State University Microscopy and NanoImaging Facility (MNIF).

Statistical analysis. Statistical analysis was carried out with JMP Pro 11, statistical software from Statistical Analysis System (SAS) Institute Inc. (Cary, NC). One-way analysis of variance (ANOVA) tests were conducted, and Tukey's HSD (honest significant difference) test was applied for multiple-pairwise comparison of samples. Significant differences were defined as having a p -value <0.05.

RESULTS AND DISCUSSION

Rheological analysis. When the elastic modulus, G' , is constant (i.e., within the linear viscoelastic region [LVR]), the sample stores the energy imparted to it and the macrostructure is not yet deformed. The average G' within the LVR is a measurement of the solid-like behavior of a sample and is used to represent gel hardness in this study. The G' of gelled yolk increased significantly ($p < 0.05$) with increasing lengths of -20 °C storage (Figure 2A), suggesting that the gel network created by freeze–thawing yolks was affected by frozen storage time. The first six time points from 0 to 28 d demonstrated an exponential increase in G' . G' of 28 and 84 d were not significantly different ($p > 0.05$), indicating that gel hardness was stabilized at these storage times. With further storage at -20 °C, gel strength increased, shown by the significant increase in G' after 84 d ($p < 0.05$). A similar trend was

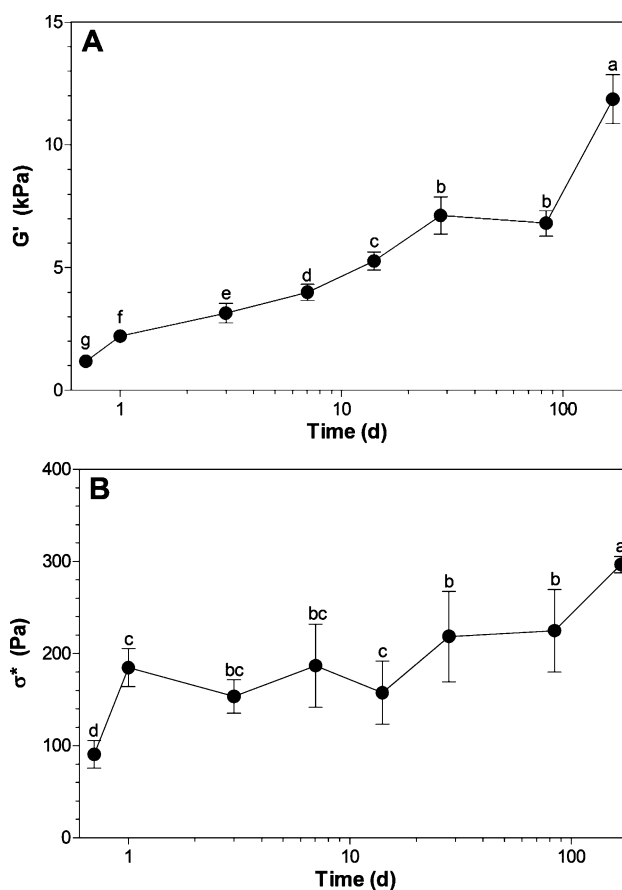


Figure 2. Elastic modulus, G' (A), and yield stress, σ^* (B), of gelled yolks stored at -20 °C for varying lengths of time (0, 1, 3, 7, 14, 28, 84, 168 d). Data point at 0.7 d is C_{0d} , 0 d gelled yolk control. Values with different letters are significantly different ($p < 0.05$).

observed in the yield stress, σ^* , of gelled yolk. Yield stress, the minimum amount of stress required to induce flow in the gelled yolk, increased significantly from 0 to 1 d and after 84 d ($p < 0.05$) but was similar in the range of 1 to 84 d (Figure 2B). It was important to determine σ^* because it is a predictor of the ease with which gelled yolk can be mixed into other ingredients during food processing, where higher σ^* corresponds to greater difficulty of mixing. Yield stress was less sensitive to storage time at -20 °C than gel hardness. For instance, G' increased 10 times after 168 d storage while yield stress increased 3 times. While the gel became significantly harder with increased storage time, the amount of force required to permanently deform the yolk was relatively stable in comparison.

Telis and Kieckbusch⁶ studied the viscoelasticity of freeze–thawed yolk with a capillary rheometer and also found that the gel structure became stronger as storage time at -20 °C increased. The longest storage time in that study was 22 h. The storage times analyzed in this study were much greater. In addition, it is possible that the gel strength continues to increase beyond 168 d, since a plateau in the G' or σ^* plot, which would indicate a stabilized gel network, was not observed. Frozen yolk has a shelf life of about 365 d, so a further study of yolks beyond 168 d should be conducted to monitor yolk structural change.

It is proposed that holding yolks for extended periods of time gave the yolk components (e.g., water, LDL, and/or granules) the opportunity to interact in such a way that a strong network

was created. The longer the frozen storage time, the greater the opportunity the components have to produce stronger, more stable gel structure, because of the continual migration and interaction of yolk components during the frozen storage. These rheological properties of gelled yolk illustrate that the yolk system is indeed a dynamic system even at $-20\text{ }^{\circ}\text{C}$.

To determine what changes are occurring in the yolk on a microscopic level, the interactions of yolk components were studied using particle size analysis, ^1H nuclear magnetic resonance spectroscopy, freezable water quantification, polyacrylamide gel electrophoresis, and transmission electron microscopy, as discussed subsequently.

Particle size analysis. Figure 3 shows the particle size distributions of fresh yolk and its two major fractions: plasma

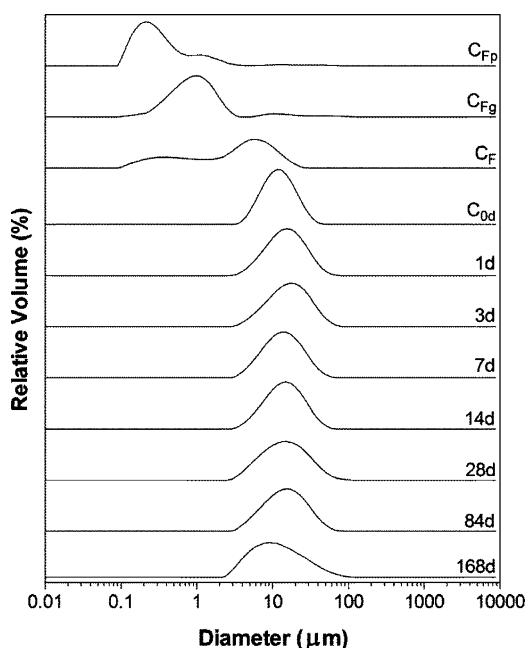


Figure 3. Representative volume weighted particle size distribution of fresh yolk fractions and fresh and gelled yolk. Gelled yolk was stored at $-20\text{ }^{\circ}\text{C}$ for varying lengths of time (1, 3, 7, 14, 28, 84, 168 d). Abbreviations are C_{Fp} , fresh yolk plasma; C_{Fg} , fresh yolk granules; C_F , fresh yolk control; C_{0d} , 0 d gelled yolk control.

and granules, as well as yolk stored at $-20\text{ }^{\circ}\text{C}$ for varying lengths of time. The plasma and granules of fresh yolk were

measured in order to identify the two populations detected in the fresh yolk control (C_F). In the particle size distribution of C_F , the population with smaller particles ranged from 0.1 to $1.3\text{ }\mu\text{m}$ in diameter with a peak population at $0.4\text{ }\mu\text{m}$, and the population with larger particles ranged from 1 to $28\text{ }\mu\text{m}$ with a peak population of $6\text{ }\mu\text{m}$. The smaller particle size population of C_F corresponded to the major population detected in the plasma fraction separated from the fresh yolk control (C_{Fp}). The particle size of C_{Fp} ranged from 0.1 to $0.8\text{ }\mu\text{m}$ with a peak population at $0.2\text{ }\mu\text{m}$. This matched the particle size distribution of pure plasma ($0.02\text{--}0.8\text{ }\mu\text{m}$, $0.25\text{ }\mu\text{m}$ peak value) measured by Strixner and Kulozik.²⁸ Therefore, LDL, the major constituent of yolk plasma, behaved similarly in fractionated plasma and in whole yolk. In contrast, the behavior of granules was different in its isolated form compared to the behavior in its native environment. The population detected in granules isolated from fresh yolk (C_{Fg}) was $0.1\text{--}4.4\text{ }\mu\text{m}$ with a peak population of $1.0\text{ }\mu\text{m}$, falling in-between the two particle populations of C_F but not matching the larger particles in fresh yolk.

LDLs are spherical particles ranging in diameter from 16 to 70 nm, and granules are $0.3\text{--}2\text{ }\mu\text{m}$ diameter circular complexes of HDL and phosvitin.^{29,30} LDLs are dispersible in aqueous systems due to their density (0.982 g/mL),³¹ and these sizes match with our TEM microstructure observations. However, our LDL size measured by particle distribution is significantly larger than that reported and microscopically observed. This may be due to a natural particle aggregation under the particle measuring conditions. In the fresh yolk under the measuring conditions, the majority of the LDL particles may have aggregated with granules, making the granule size much larger than that in its isolated stage. As a result, the LDL particle population intensity is also greatly reduced.

There were three major changes in the particle size distribution of yolks stored at $-20\text{ }^{\circ}\text{C}$ for varying lengths of time. Differences were observed between the following groupings: C_F vs all gelled yolks (C_{0d} and 1–168 d), 0 d vs 1–84 d, and 168 d vs all other samples. C_F had two populations whereas all gelled yolks had one population with larger particle sizes (Figure 3 and Table 1). In Figure 3, the general shapes of the curves of 1, 3, 28, and 84 d samples were different from that of 7 and 14 d, which had narrower distributions. In 168 d, there was a shift in the distribution of particle size that was not observed in any other sample. The highest frequency, or peak of the curve, decreased in 168 d, whereas it increased in all

Table 1. Percentile Diameters, Surface Area Moment Mean, and Volume Moment Mean of Fresh and Gelled Yolk^a

	$d(0.1)^b$	$d(0.5)^b$	$d(0.9)^b$	$D[3, 2]^c$	$D[4, 3]^d$
C_F^e	$0.31 \pm 0.01\text{ f}$	$4.21 \pm 0.26\text{ e}$	$11.95 \pm 0.46\text{ c}$	$1.00 \pm 0.03\text{ e}$	$5.21 \pm 0.22\text{ e}$
C_{0d}^f	$5.95 \pm 0.01\text{ d}$	$11.13 \pm 0.02\text{ d}$	$20.98 \pm 0.11\text{ b}$	$9.97 \pm 0.01\text{ d}$	$12.51 \pm 0.04\text{ d}$
1d	$7.54 \pm 0.17\text{ a}$	$16.76 \pm 0.71\text{ ab}$	$34.97 \pm 1.95\text{ a}$	$13.92 \pm 0.43\text{ a}$	$19.43 \pm 0.89\text{ ab}$
3d	$7.30 \pm 0.24\text{ ab}$	$17.29 \pm 0.83\text{ a}$	$37.83 \pm 2.13\text{ a}$	$13.97 \pm 0.50\text{ a}$	$20.44 \pm 0.95\text{ a}$
7d	$6.74 \pm 0.14\text{ c}$	$15.00 \pm 0.61\text{ c}$	$32.57 \pm 3.14\text{ a}$	$12.51 \pm 0.19\text{ bc}$	$17.76 \pm 1.12\text{ bc}$
14d	$7.01 \pm 0.14\text{ bc}$	$15.30 \pm 0.18\text{ bc}$	$32.04 \pm 1.25\text{ a}$	$12.84 \pm 0.09\text{ bc}$	$17.80 \pm 0.40\text{ bc}$
28d	$6.32 \pm 0.12\text{ d}$	$15.16 \pm 0.72\text{ bc}$	$36.24 \pm 2.16\text{ a}$	$12.30 \pm 0.41\text{ c}$	$18.83 \pm 0.98\text{ ab}$
84d	$6.94 \pm 0.12\text{ bc}$	$16.52 \pm 0.97\text{ abc}$	$36.99 \pm 3.47\text{ a}$	$13.34 \pm 0.44\text{ ab}$	$19.73 \pm 1.41\text{ ab}$
168d	$4.81 \pm 0.03\text{ e}$	$11.66 \pm 0.04\text{ d}$	$33.84 \pm 0.93\text{ a}$	$9.60 \pm 0.01\text{ d}$	$16.32 \pm 0.27\text{ c}$

^aGelled yolks were stored at $-20\text{ }^{\circ}\text{C}$ for varying lengths of time (1, 3, 7, 14, 28, 84, 168 d). Values with different letters within each column are significantly different ($p < 0.05$). ^b $d(0.1)$, $d(0.5)$, and $d(0.9)$; 10%, 50%, and 90% of the volume distribution, respectively, are below this value. ^c $D[3, 2]$, surface area moment mean (Sauter Mean Diameter). ^d $D[4, 3]$ is volume moment mean (De Brouckere Mean Diameter). ^e C_F , fresh yolk control. ^f C_{0d} , gelled yolk control.

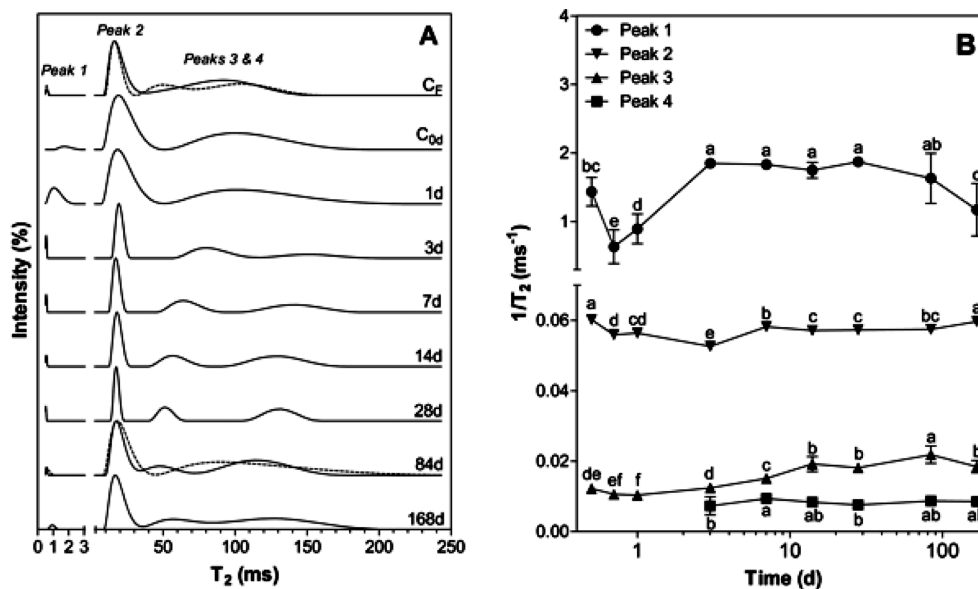


Figure 4. Representative CPMG spectra (A) and spin–spin relaxation rate (B) of fresh and gelled yolk. Gelled yolk was stored at $-20\text{ }^{\circ}\text{C}$ for varying lengths of time (1, 3, 7, 14, 28, 84, 168 d). Abbreviations of Figure 4A are C_F , fresh yolk control; C_{0d} , 0 d gelled yolk control. Dashed lines of C_F and 84d represent observation of three peaks for half of the measurements of sample and four peaks for the other half. Figure 4B data point at 0.5 d is C_F , fresh yolk control; data point at 0.7 d is C_{0d} , 0 d gelled yolk control.

other gelled yolk samples relative to C_F and C_{0d} . Thus, the diameter of the majority of yolk particles increased in all gelled yolk samples compared to C_F and C_{0d} but decreased from 84 to 168 d. This trend was seen in the surface area and volume moment mean (D [3, 2] and D [4, 3], respectively) of the aforementioned sample groupings (Table 1). The volume moment mean was especially important because it reflects the size of particles that constitute the majority of the sample volume.³² It is most sensitive to large particles and was therefore a crucial measurement when considering the hypothesis that gelation results from the formation of larger particles caused by aggregation of LDL or apolipoproteins during freeze–thawing. The surface area moment mean must not be neglected, as it is most sensitive to fine particulates³² and was crucial in monitoring the proportion of smaller particles (i.e., unaggregated LDL) present.

Table 1 shows that C_F had the highest abundance of smaller particles, or smallest percentile diameters, compared to all gelled yolk samples. Significant increases in d (0.1), d (0.5), d (0.9), D [3, 2], and D [4, 3] were observed early in frozen storage, between C_F , C_{0d} and 1d samples ($p < 0.05$) (Table 1). As fresh yolk transitioned to zero storage gelled yolk and then 1 d gelled yolk, the particle size distribution shifted significantly toward particles with larger diameters. The same trend was observed in particle size results across all samples. The percentile diameters, surface area moment mean, and volume moment mean decreased slightly from 3 to 7 d, remained constant at 14 d, increased slightly at 84 d, and finally decreased considerably at 168 d. These changes were statistically different (Table 1) and somewhat related to the changes observed in yield stress of the samples. Particle size has direct influence on material properties such as viscosity, flowability, and texture.³² In gelled yolks, particle size appeared to have a direct influence on the force required to change the solid-like behavior of the gel into that of a viscous liquid.

The particle size distribution of gelled yolk shifted toward a greater population of larger particles after longer storage times

at $-20\text{ }^{\circ}\text{C}$, as indicated by the significant increase ($p < 0.05$) of specific surface area and volume mean (Table 1). Accordingly, the yield stress of gelled yolk increased significantly after the first day of frozen storage (Figure 2B). At 168 d, σ^* of 300 Pa was significantly greater than others ($p < 0.05$). However, both particle size values of 168 d unexpectedly decreased significantly. This suggested the release of smaller particles or dissociation of the aggregates among LDL and/or granule particles. These smaller particles may have dissociated from the gel network after storage at >84 d at $-20\text{ }^{\circ}\text{C}$, and they may have helped strengthen the gel network by forming additional linkages and interactions. The interpretation of changes observed in rheological and particle size analyses was further validated by studying yolk at the nano and micrometer levels, particularly yolk matrix mobility using ^1H NMR spectroscopy, protein changes with PAGE, and gel network rearrangement with TEM.

Matrix mobility. Figure 4 shows the overall variation in the matrix of fresh and gelled yolk samples based on changes in spin–spin relaxation times (T_2) and proton populations (PP, i.e. % intensity) of the 3–4 proton pools detected in egg yolk. In a previous study, Au³³ interpreted the appearance of four peaks in half of the replicated measurements of only certain samples (C_F and 84 d in this study). The spectrometer may not have been able to distinguish the two most mobile proton pools some of the time due to the complexity of the egg yolk system. It is also possible that the yolk matrix is very heterogeneous, and thus slight changes in matrix mobility can be observed among sample replicates. The proton pools were identified from the least to most mobile (smallest to largest T_2) as protons from Peak 1, protein and interactions between protein, lipid, and water; Peaks 2 and 3, lipid and lipid–water interactions; and Peak 4, unbound water or exchangeable protons of protein or lipid.³³

The length of frozen storage at $-20\text{ }^{\circ}\text{C}$ had a significant effect on T_2 and PP of all proton pools of yolk, with the greatest changes occurring when comparing the following groupings:

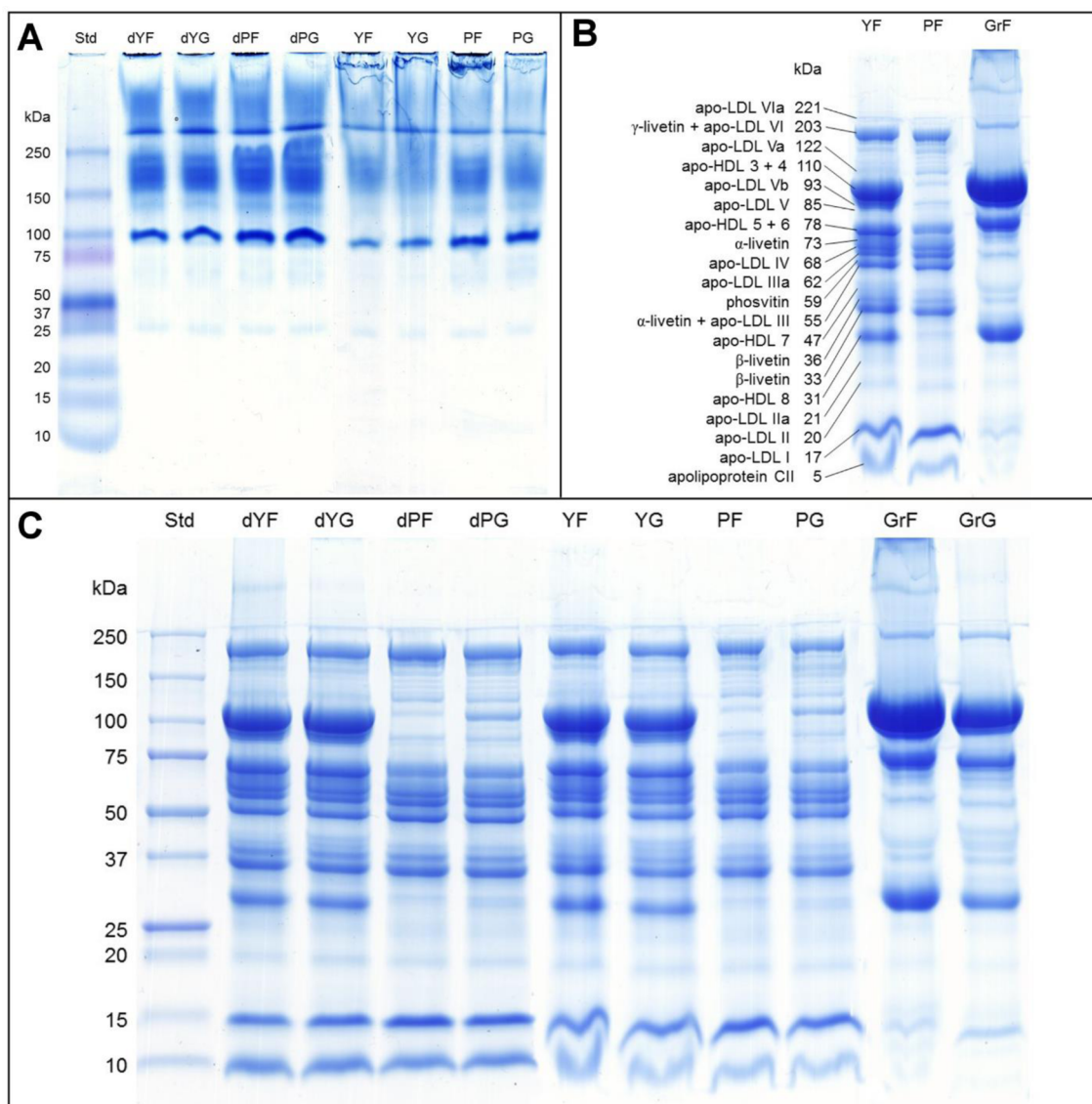


Figure 5. Native-PAGE of yolk and plasma (A), SDS-PAGE of yolk, plasma, and granules with identified proteins (B), and SDS-PAGE of yolk, plasma, and granules (C). Proteins were identified based on SDS-PAGE profiles by Guilmineau et al.⁴⁶ Abbreviations are Std, standard; d, delipidated; Y, yolk; P, plasma; Gr, granules; F, fresh; G, gelled.

C_F , C_{0d} , and 1 d; 3–28 d; and 84–168 d (Figure 4A, Table S1 of the Supporting Information). The most notable difference among the three groups was the presence of four peaks in samples stored for >3 d. From 3 to 28 d, the two most mobile proton pools (Peaks 3 and 4) showed continuous decrease in T_2 (i.e., less mobile) and increase in peak resolution (Figure 4A). T_2 was expected to continue decreasing and peak resolution was expected to continue increasing according to this trend. However, at 84 and 168 d, the two proton pools lost peak resolution, and the T_2 did not change with increasing storage time. This is a very interesting change with longer storage time, and it deserves a further investigation. It seems that the most mobile proton pools (Peaks 3 and 4) which represent unbound water and/or exchangeable protons of protein or lipid are becoming more mobile and less differentiated.

In foods, water is typically described as bulk water or bound water. The concept of free and bound water is key to understanding matrix mobility of food systems, but it is

inaccurate to describe water only as such. Water does not exist as two discrete states. There is a continuum of free and bound water in food systems where many layers of water molecules form around macromolecules.^{34,35} The water layers furthest from the macromolecule have the highest mobility while the layers directly participating in hydrogen bonding with hydrophilic sites on the macromolecule have the lowest mobility.^{34,36}

The increased peak resolution of the two most mobile proton pools from 3 to 28 d (Figure 4A) suggests that the continuum of bound and free water became more distinct as frozen storage time increased. Aggregation of yolk components such as LDL, HDL, and apolipoproteins may explain the changes in the status of water over time. It is hypothesized that LDLs aggregate due to protein–protein interaction among the disrupted apolipoproteins caused by slow freezing. The removal of water results in the concentration of nonwater molecules which is conducive to LDL aggregation. At shorter frozen storage times, some removal of the water causes aggregation of yolk components. Extended storage at freezing temperatures

below -6°C provides the yolk matrix time to reorganize into a more stable conformation. Continuous removal of free water may have contributed to rearrangement of LDL and/or HDL so that the yolk system will possess the lowest potential energy. After 28 d of frozen storage, particles continued to aggregate, small particles were released, and therefore, water became again trapped within the particle network. As the surface area of the network increased, the likelihood of interaction between water molecules and apolipoproteins increased. As these interactions increased with longer frozen storage, more and more previously freed water became bound within the lipoprotein network, as shown in 84 and 168 d samples. Previous studies^{37,38} on milk protein aggregation used a similar technique and demonstrated protein aggregation.

The evolution of spin–spin relaxation rate ($1/T_2$) of fresh and gelled yolk components (Peaks 1–4) is shown in Figure 4B. Overall, it was clear that T_2 rate of all yolk components was dependent on the length of storage at -20°C . The relaxation rate of Peak 3, the lipid–water proton pool, increased with the increase of frozen storage time. The lipid–water protons relaxed quicker as storage time increased, so they became less mobile. Peaks 1 and 2 had the same pattern for the first three time points ($1/T_2$ decreased from C_F to C_{0d} then increased slightly at 1 d), but different relationship was observed 3–168d. The relaxation rate of Peak 1, or the protein/protein–water pool, increased at 3 d, stabilized until 28 d, and then decreased slightly from 84 to 168 d. The lipid/lipid–protein protons of Peak 2 showed the opposite trend, where the relaxation rate decreased at 3d, stabilized until 28 d, and then increased from 84 to 168 d. This relationship indicates the exchange of protein and lipid protons during freezing storage. Yolk gelation is a result not just of changes in water and lipoprotein particle interactions but also interactions between yolk proteins and lipids. This interpretation still supports the lipoprotein particle aggregation hypothesis, as disruption and conformational changes of apolipoproteins would affect the relaxation rates of protein and lipid. This is the first time such matrix mobility technique was used to study the kinetics of yolk gelation.

Free water content. The matrix mobility experiment determined that water molecules of yolk were greatly affected by the length of frozen storage. To confirm the observed changes in bound and unbound water of yolk, the unbound water content was studied according to the method of Wakamatu et al.²⁴ However, none of the freezable water content were statistically different in fresh and gelled yolk for all frozen storage time treatments. The DSC method was determined to be not sensitive enough to distinguish the minute changes in water states that the ^1H NMR spectrometer detected.

Protein characterization. Plasma and granule fractions were prepared to differentiate yolk proteins. PAGE analysis of the plasma and granules helped determine which fractions participated in freeze–thaw gelation by observing changes in the protein bands in various samples.

The interference at the top of the Native-PAGE gel in the lanes of fresh and gelled yolk (YF and YG) and plasma (PF and PG) samples was caused by lipids because the defect was not present in delipidated samples (dYF, dYG, dPF, and dPG) (Figure 5A). Therefore, only delipidated samples are considered in this discussion. There was no obvious difference in the band pattern of dYF and dYG aside from more extreme downward curving, or frowning, of the 100 kDa (kDa) band in the gelled yolk. Frowning may indicate overloading of

protein,³⁹ so there may be a higher concentration of 100 kDa protein in gelled yolk. Aggregation may have occurred through increased disulfide bonding events during gelation, as disulfide bonds are a source of frowning or streaking in PAGE.^{40–42} The HDL of granules contain the majority (86%) of the cysteine residues that would be available for disulfide bond formation.⁴³ Densitometric analysis of the bands confirmed a significant increase ($p < 0.05$) in the optical density (OD) of the 100 kDa band when comparing fresh and gelled samples (Table S2). The Native gel protein profiles are very different from that of SDS-PAGE (Figures 5B and C) which are reported in most studies. Anton's group also reported Native-PAGE for yolk proteins,^{44,45} and the general protein profiles are very similar to ours. We intended to study if there was protein aggregation due to freeze-induced gelation using Native-PAGE, however, the Native condition does not give well-defined protein separation as needed.

Figure 5B shows the SDS-PAGE profiles of fresh yolk (YF), plasma from fresh yolk (PF), and granules from fresh yolk (GrF). All major yolk proteins identified by Guilmineau et al.⁴⁶ matched those observed in Figure 5B and were identified as such. Bands of 33, 36, 55, and 73 kDa (livetins) and 5–21, 55, 62, 68, and 122 kDa (apo-LDL) were confirmed as plasma proteins by noting the presence of the bands in PF and their absence in GrF. The same was observed for bands of 59 kDa (phosvitin) and 31, 47, 78, and 110 kDa which are apo-HDL proteins.

Delipidation of yolk and plasma did not affect the density or electrophoretic mobility of the proteins in yolk and plasma on SDS-PAGE, though delipidation gave better separation and minimal warping of lower MW proteins (5 and 17 kDa). As a result, only the delipidated fresh and gelled yolk (dYF and dYG) and plasma (dPF and dPG) samples are considered in this discussion of SDS-PAGE protein analysis. The granules of fresh and gelled yolk (GrF and GrG) are included in Figure 5C to show that some of the granular proteins (31, 78, and 110 kDa apo-HDL) were not completely extracted from gelled yolk. This resulted in the greater OD of 31, 78, and 110 kDa apo-HDL in plasma collected from gelled compared to fresh yolk (Figure 5C).

Several differences in SDS-PAGE profiles were observed in dYF and dYG. A very high MW protein (>270 kDa) observed in granules had greater OD in dYF compared to dYG (Figure 5C, Table S3), suggesting that the protein belonged to the granular fraction in a complex and it dissociated during gelation. The >270 kDa protein complex may have dissociated into 47 kDa subunits, as the 47 kDa band in dYG had significantly greater OD compared to dYF (Figure 5C, Table S3). The 47 kDa subunits may be apo-HDL (Figure 5B) found in the granules of yolk. Furthermore, the >270 kDa band was present in GrF but not in GrG, and the 47 kDa band with greater OD in dYG was also seen in GrG. This supports the hypothesis that after freeze–thaw, the >270 kDa complex dissociated into 47 kDa subunits and that both proteins were part of the granular fraction.

In dPF and dPG, there was also a marked difference in the OD of granular proteins apo-HDL 3 + 4 with molecular weights of ~ 110 kDa. The 110 kDa band had significantly greater OD ($p < 0.05$) in dPG compared to in dPF, as well as in dYG vs dYF (Table S3). This indicates that a larger amount of 110 kDa apo-HDL was separated into the supernatant as plasma after gelation. The plasma from gelled yolk also had higher intensity of the 31 and 78 kDa HDL protein bands than

plasma from fresh yolk. This is a critical observation to support that granules or subfractions of granules are involved in gelation by forming a strong LDL-granule interaction. Such interaction is likely a hydrophobic one because the Native-PAGE did not show a higher molecular weight protein band in either PG or dPG sample compared to their fresh yolk counterparts. Past studies have emphasized the key role of plasma LDL but not granules in the gelation mechanism,^{4,7,9,10,15,24} yet our results agreed with some studies that suggest gelation may involve compounds other than LDL.^{8,13,47}

Microstructure. The electron micrographs in this study resembled those of Mineki and Kobayashi.²⁷ The shapes and electron densities of the yolk structures were comparable, and the size and shape of granules reported (0.3–2.5 μm dia) were similar to the granules observed in our study. Plasma LDL and granules were identified based on their size and composition. Granules were the large, dark gray bodies of 0.2–3 μm dia (Figure 6). LDLs were the numerous smaller, dark gray bodies with diameters of approximately 10–30 nm observed in the matrix surrounding the granules. Based on their high electron density and known composition (64% protein), the granules were regarded as proteins. LDLs were identified due to their staining characteristics and known composition of ~86% lipids. Lipids, which are stained and fixed by osmium tetroxide, appear

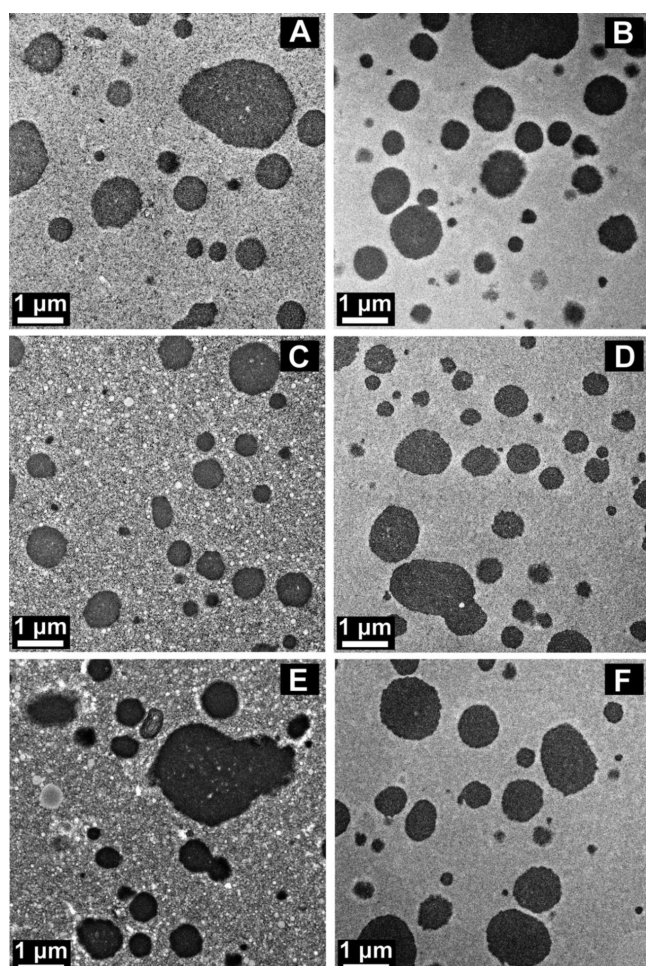


Figure 6. TEM micrographs of osmicated and nonosmicated fresh and gelled yolk. Samples are osmicated fresh (A), nonosmicated fresh (B), osmicated 1 d gelled (C), nonosmicated 1 d gelled (D), osmicated 168 d gelled (E), nonosmicated 168 d gelled (F) yolk.

electron-dense. If samples are not osmicated, lipids are removed from subsequent preparation steps. By preparing yolk samples with and without osmication, the lipids particles were identified. In Figure 6, the left column of images (A, C, and E) show osmicated samples with many small dark bodies in the matrix, while the images in the right column (B, D, and F) are nonosmicated and lack the small bodies.

The most notable changes in yolk microstructure were observed between fresh yolk (Figure 6A) and yolk stored at $-20\text{ }^{\circ}\text{C}$ for 1 d (Figure 6C) and 168 d (Figure 6E). After 1 d of frozen storage, the yolk matrix was disrupted by voids with little to no electron density (Figure 6C). Hasiak et al.⁴⁸ noted the same effect after 3 d freezing and thawing of yolk. However, there were no marked differences in the appearance of gelled yolk stored >1 d until 168 d of frozen storage (Figure 6E, Figure S1 of the Supporting Information). The voids became less uniform in shape, with more appearing around the edge of the granules. Furthermore, there was an increase in the appearance of small, electron-translucent regions within the granules (Figure 6E). These results indicated two important changes in yolk during freezing and thawing. The voids were likely due to ice crystal growth, as a previous microscopy study showed that voids in egg yolk indicated ice crystal damage.⁴⁹ This suggests that as yolk froze, microscopic ice crystals disrupted the matrix. In addition, the appearance of the electron translucent regions within the granules may indicate that granular components became dissociated during freezing, particularly after a long period of frozen storage such as >84 d.

Proposed two-stage gelation process. Constituents of both plasma and granules of egg yolk contribute to freeze–thaw yolk gelation. Evidence shows that there are two stages of gelation during prolonged frozen storage. The proposed mechanism is shown in Figure 7. The first stage, observed from 1 to 28 d of storage at $-20\text{ }^{\circ}\text{C}$, involves the aggregation of

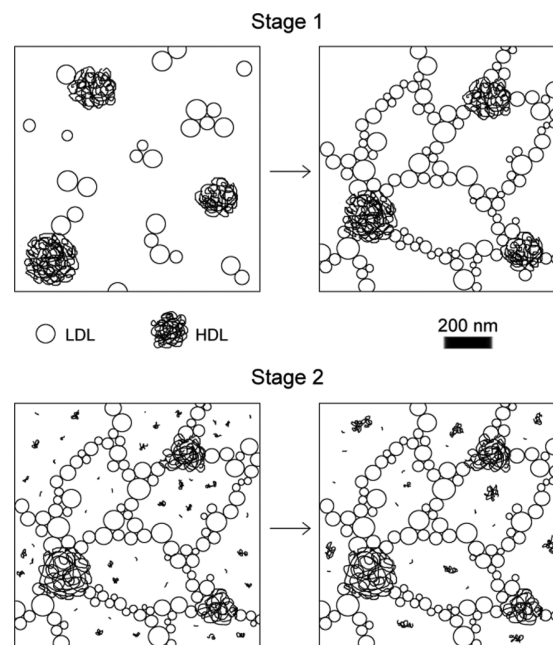


Figure 7. Schematic representation of the proposed mechanism of two-stage yolk gelation during prolonged freeze storage. The non-denoted particles in Stage 2 illustrations are the released proteins or lipoproteins self-associated or associating with the previously formed network.

lipoprotein particles via hydrophobic interactions resulting from the water removal during slow freezing. The granules or HDL particles are also involved in aggregation. States of water continue to change as the gel network stabilizes with increased length of freezing. At a certain point, between 28 and 84 d, the second stage of gelation begins. It is hypothesized that proteins or particles that were previously participating in the first stage of gelation are released. Such dissociated proteins are now more mobile, and the increased surface area exposes more binding sites providing further self-association or with the previously formed network, strengthening the gel. This second stage gelation is explained by the matrix mobility changes and the particle size distribution changes. Granules, specifically 47 and 110 kDa apo-HDL, were shown to play a role in gelation. This proposed two-stage gelation process is a putative mechanism and the model needs further validation.

Summary. Many studies have been published demonstrating the role of plasma LDL in the freeze–thaw gelation of yolk, but granules should not be disregarded in determining the mechanism of gelation. In this study, both plasma and granules were shown to contribute to gelation with the use of techniques that are common and unique for this study. These methods allowed for the successful evaluation of yolk gel strength, particle size, matrix mobility, protein aggregation, and microstructure as influenced by long-term freezing storage. In particular, the proposed dynamic and two-stage gelation described in this study has never been reported. This is important because it could indicate that the yolk system is dynamic even at $-20\text{ }^{\circ}\text{C}$, and macro- and nanoscopic changes continue during long-term freeze storage up to 168 d. The proposed two-stage gelation mechanism needs further validation with even longer time of storage.

■ ASSOCIATED CONTENT

📄 Supporting Information

The Supporting Information is available free of charge on the ACS Publications website at DOI: [10.1021/acs.jafc.5b04109](https://doi.org/10.1021/acs.jafc.5b04109).

T_2 , PP, and peak resolution of fresh and gelled yolk; TEM micrographs of gelled yolk; Optical Density of Native-PAGE Yolk Protein Bands; Optical Density of SDS-PAGE Yolk Protein Bands ([PDF](#))

■ AUTHOR INFORMATION

Corresponding Authors

*(T.W.) Tel.: 515-294-5448; fax: 515-294-8181. E-mail: tongwang@iastate.edu.

*(N.C.A.) Tel.: 515-294-5962; fax: 515-294-8181. E-mail: nacevedo@iastate.edu.

Funding

This material is based upon work supported by the National Institute of Food and Agriculture, U.S. Department of Agriculture, under Award No. 2015-67017-23115. Any opinions, findings, conclusions, or recommendations expressed in this publication are those of the author(s) and do not necessarily reflect the view of the U.S. Department of Agriculture.

Notes

The authors declare no competing financial interest.

■ REFERENCES

- (1) Kiosseoglou, V. Egg yolk protein gels and emulsions. *Curr. Opin. Colloid Interface Sci.* **2003**, *8*, 365–370.
- (2) McKee, S. Egg product functionality. http://www.aeb.org/images/website/documents/food-manufacturers/order-aeb-resources/Functionality_of_Eggs_in_Baked_Goods.ppt (accessed Jan 1, 2015).
- (3) Moran, T. The effect of low temperature on hens' eggs. *Proc. R. Soc. London, Ser. B* **1925**, *98*, 436–456.
- (4) Powrie, W. D.; Little, H.; Lopez, A. Gelation of egg yolk. *J. Food Sci.* **1963**, *28*, 38–46.
- (5) American Egg Board (AEB). All about egg products: processing, handling & storage. <http://www.aeb.org/food-manufacturers/all-about-egg-products/processing-handling-a-storage> (accessed November 13, 2013).
- (6) Telis, V. R. N.; Kieckbusch, T. G. Viscoelasticity of frozen/thawed egg yolk. *J. Food Sci.* **1997**, *62*, 548–550.
- (7) Kurisaki, J. I.; Kaminogawa, S.; Yamauchi, K. Studies of freeze-thaw gelation of very low density lipoprotein from hen's egg yolk. *J. Food Sci.* **1980**, *45*, 463–466.
- (8) Wakamatu, T.; Sato, Y.; Saito, Y. Identification of the components responsible for the gelation of egg yolk during freezing. *Agric. Biol. Chem.* **1982**, *46*, 1495–1503.
- (9) Kumar, S. A.; Mahadevan, S. Physicochemical studies on the gelation of hen's egg yolk: Delipidation of yolk plasma by treatment with phospholipase-C and extraction with solvents. *J. Agric. Food Chem.* **1970**, *18*, 666–670.
- (10) Mahadevan, S.; Satyanarayana, T.; Kumar, S. A. Physicochemical studies on the gelation of hen egg yolk: separation of gelling protein components from yolk plasma. *J. Agric. Food Chem.* **1969**, *17*, 767–771.
- (11) Saari, A.; Powrie, W. D.; Fennema, O. Influence of freezing egg yolk plasma on the properties of low-density lipoproteins. *J. Food Sci.* **1964**, *29*, 762–765.
- (12) Sato, Y.; Takagaki, Y. Influence of thawing rate and aging temperature on viscosity of freeze-thawed yolk and low density lipoprotein. *Agric. Biol. Chem.* **1976**, *40*, 49–55.
- (13) Chang, C. H.; Powrie, W. D.; Fennema, O. Studies on the gelation of egg yolk and plasma upon freezing and thawing. *J. Food Sci.* **1977**, *42*, 1658–1665.
- (14) Jaax, S.; Travnicek, D. The effect of pasteurization, selected additives and freezing rate on the gelation of frozen-defrosted egg yolk. *Poult. Sci.* **1968**, *47*, 1013–1022.
- (15) Meyer, D. D.; Woodburn, M. Gelation of frozen-defrosted egg yolk as affected by selected additives: viscosity and electrophoretic findings. *Poult. Sci.* **1965**, *44*, 437–446.
- (16) Huang, L.; Wang, T.; Han, Z.; Lu, X. Effect of egg yolk freezing on properties of mayonnaise. Revision is currently being evaluated, 2015.
- (17) McBee, L. E.; Cotterill, O. J. Ion-exchange chromatography and electrophoresis of egg yolk proteins. *J. Food Sci.* **1979**, *44*, 656–667.
- (18) Anton, M. Egg yolk: structures, functionalities and processes. *J. Sci. Food Agric.* **2013**, *93*, 2871–2880.
- (19) Cham, B. E.; Knowles, B. R. A solvent system for delipidation of plasma or serum without protein precipitation. *J. Lipid Res.* **1976**, *17*, 176–181.
- (20) Beekman, A.; Shan, D.; Ali, A.; Dai, W.; Ward-Smith, S.; Goldenberg, M. Micrometer-scale particle sizing by laser diffraction: critical impact of the imaginary component of refractive index. *Pharm. Res.* **2005**, *22*, 518–522.
- (21) Kralik, G.; Kralik, Z.; Suchý, E.; Straková, D. Effects of dietary selenium source and storage on internal quality of eggs. *Acta Vet. Brno* **2009**, *78*, 219–222.
- (22) Provencher, S. W. CONTIN: A general purpose constrained regularization program for inverting noisy linear algebraic and integral equations. *Comput. Phys. Commun.* **1982**, *27*, 229–242.
- (23) Kamat, V.; Graham, G.; Barratt, M.; Stubbs, M. Freeze–thaw gelation of hen's egg yolk low density lipoprotein. *J. Sci. Food Agric.* **1976**, *27*, 913–927.
- (24) Wakamatu, T.; Sato, Y.; Saito, Y. On sodium chloride action in the gelation process of low density lipoprotein (LDL) from hen egg. *J. Food Sci.* **1983**, *48*, 507–512.

- (25) Laca, A.; Paredes, B.; Díaz, M. A method of egg yolk fractionation: characterization of fractions. *Food Hydrocolloids* **2010**, *24*, 434–443.
- (26) National Institute of Health (NIH). Optical density calibration. <http://rsb.info.nih.gov/ij/docs/examples/calibration/index.html> (accessed Mar 8, 2015).
- (27) Mineki, M.; Kobayashi, M. Microstructure of yolk from fresh eggs by improved method. *J. Food Sci.* **1997**, *62*, 757–761.
- (28) Strixner, T.; Kulozik, U. Continuous centrifugal fractionation of egg yolk granules and plasma constituents influenced by process conditions and product characteristics. *J. Food Eng.* **2013**, *117*, 89–98.
- (29) Chang, C. M.; Powrie, W. D.; Fennema, O. Microstructure of egg yolk. *J. Food Sci.* **1977**, *42*, 1193–1200.
- (30) Bellairs, R. The structure of the yolk of the hen's egg as studied by electron microscopy: I. The Yolk of the Unincubated Egg. *J. Cell Biol.* **1961**, *11*, 207–225.
- (31) Anton, M. Low-density lipoproteins (LDL) or lipovitellenin fraction. In *Bioactive egg compounds*; Anton, M., Huopalahti, R., Lopez-Fandino, R., Schade, R., Eds.; Springer: Heidelberg, Germany, 2007; pp 7–12.
- (32) Malvern. *A basic guide to particle characterization*; Malvern Instruments Limited: Worcestershire, UK, 2012; pp 1–26.
- (33) Au, C. *Determination of the gelation mechanism of freeze-thawed hen egg yolk*. M.S. Thesis, Iowa State University, 2015.
- (34) Ruan, R. R.; Chen, P. L. Aspects of water in food and biological systems. In *Water in foods and biological materials: a nuclear magnetic resonance approach*; Technomic Pub. Co.: Lancaster, PA, 1998; pp 51–74.
- (35) Muffett, D. J. *Bound and free water relationships in soy proteins as measured by differential scanning calorimetry*. Ph.D. Thesis, Iowa State University, 1979.
- (36) Hills, B. P.; Tackacs, S. F.; Belton, P. S. A new interpretation of proton NMR relaxation time measurements of water in food. *Food Chem.* **1990**, *37*, 95–111.
- (37) Indrawati, L.; Stroshine, R. L.; Narsimhan, G. Low-field NMR: A tool for studying protein aggregation. *J. Sci. Food Agric.* **2007**, *87*, 2207–2216.
- (38) Aymard, P.; Gimel, J. C.; Nicolai, T.; Durand, D. Experimental evidence for a two-step process in the aggregation of α -lactoglobulin at pH 7. *J. Chim. Phys.-Chim. Biol.* **1996**, *93*, 987–994.
- (39) Bio-Rad. Performing electrophoresis: evaluation of separation. <http://www.bio-rad.com/en-us/applications-technologies/performing-protein-electrophoresis#4> (accessed March 14, 2015).
- (40) Nybo, K. Native PAGE. *BioTechniques* **2012**, *52*, 10.2144/000113797.
- (41) Rajagopal, K.; Gowda, C.; Singh, P. Diffusion, Frowning and smiling of low molecular weight protein bands: a simple, rapid and efficient solution. *Int. J. Pept. Res. Ther.* **2015**, *21*, 7–11.
- (42) Cumming, R. C.; Andon, N. L.; Haynes, P. A.; Park, M.; Fischer, W. H.; Schubert, D. Protein disulfide bond formation in the cytoplasm during oxidative stress. *J. Biol. Chem.* **2004**, *279*, 21749–21758.
- (43) Cook, W. H.; Burley, R. W.; Martin, W. G.; Hopkins, J. W. Amino acid compositions of the egg-yolk lipoproteins, and a statistical comparison of their amino acid ratios. *Biochim. Biophys. Acta* **1962**, *60*, 98–103.
- (44) Le Denmat, M.; Anton, M.; Gandemer, G. Protein denaturation and emulsifying properties of plasma and granules of egg yolk as related to heat treatment. *J. Food Sci.* **1999**, *64*, 194–197.
- (45) Anton, M.; Le Denmat, M.; Gandemer, G. Thermostability of hen egg yolk granules: Contribution of native structure of granules. *J. Food Sci.* **2000**, *65*, 581–584.
- (46) Guilmineau, F.; Krause, I.; Kulozik, U. Efficient analysis of egg yolk proteins and their thermal sensitivity using sodium dodecyl sulfate polyacrylamide gel electrophoresis under reducing and nonreducing conditions. *J. Agric. Food Chem.* **2005**, *53*, 9329–9336.
- (47) Soliman, F. S.; Van Den Berg, L. Factors affecting freeze aggregation of lipoprotein. *Cryobiology* **1971**, *8*, 265–270.
- (48) Hasiak, R. J.; Vadehra, D. V.; Baker, R. C.; Hood, L. Effect of certain physical and chemical treatments on the microstructure of egg yolk. *J. Food Sci.* **1972**, *37*, 913–917.
- (49) Woodward, S. A.; Cotterill, O. J. Preparation of cooked egg white, egg yolk, and whole egg gels for scanning electron microscopy. *J. Food Sci.* **1985**, *50*, 1624–1628.